Eidgenössische Technische Hochschule Zürich

Ecole polytechnique fédérale de Zurich
Politecnico federale di Zurigo
Swiss Federal Institute of Technology Zurich

Domain decomposition preconditioners of Neumann-Neumann type for *hp*-approximations on boundary layer meshes in three dimensions*

A. Toselli and X. Vasseur

Research Report No. 2003-01
January 2003

Seminar für Angewandte Mathematik
Eidgenössische Technische Hochschule
CH-8092 Zürich
Switzerland

*This work was partially supported by the Swiss National Science Foundation under Project 20-63397.00

Domain decomposition preconditioners of Neumann-Neumann type for *hp*-approximations on boundary layer meshes in three dimensions*

A. Toselli and X. Vasseur

Seminar für Angewandte Mathematik
Eidgenössische Technische Hochschule
CH-8092 Zürich
Switzerland

Research Report No. 2003-01 January 2003

Abstract

We develop and analyze Neumann-Neumann methods for *hp* finite element approximations of scalar elliptic problems on geometrically refined boundary layer meshes in three dimensions. These are meshes that are highly anisotropic where the aspect ratio typically grows exponentially with the polynomial degree. The condition number of our preconditioners is shown to be independent of the aspect ratio of the mesh and of potentially large jumps of the coefficients. In addition, it only grows polylogarithmically with the polynomial degree, as in the case of p approximations on shape-regular meshes. This work generalizes our previous one on two-dimensional problems in [40,42] and the estimates derived here can be employed to prove condition number bounds for certain types of FETI methods.

Keywords: Domain decomposition, preconditioning, *hp* finite elements, spectral elements, anisotropic meshes

Subject Classification: 65N22, 65N55, 65N35

*This work was partially supported by the Swiss National Science Foundation under Project 20-63397.00

1 Introduction

Solutions of elliptic boundary value problems in polyhedral domains have corner and edge singularities and, in addition, boundary layers may also arise in laminar, viscous, incompressible flows with moderate Reynolds numbers at faces, edges, and corners. Suitably graded meshes, geometrically refined towards corners, edges, and/or faces, can be employed in order to achieve an exponential rate of convergence of *hp* finite element approximations; see, e.g., [4, 5, 26, 36, 37].

Neumann-Neumann (NN) and FETI algorithms are particular iterative substructuring methods and are among the most popular and heavily tested domain decomposition (DD) methods; see, e.g, [19, 13, 24, 7]. Unfortunately, the performance of iterative substructuring methods might be severely compromised if very thin elements and/or subdomains or general non quasiuniform meshes are employed.

Some work has been done on domain decomposition preconditioners for higher order approximations of three-dimensional problems. It is well-known that on shape-regular meshes special care must be taken in the choice of the basis functions in order to produce preconditioners that are robust with respect to the polynomial degree. We mention, e.g., [21, 22, 23, 29, 8, 38]. For p approximations that employ nodal basis functions on Gauss-Lobatto nodes (spectral element approximations), many iterative substructuring methods can be successfully employed and studied; see [33, 34, 30, 32] and the references therein. Some of these ideas can be and have been generalized to *hp* approximations. We mention, e.g., [2, 1, 28, 14, 20, 3, 18] and the references therein and, in particular, [15] for three-dimensional problems. In all the above-mentioned works, however, the finite element mesh is assumed to be shape-regular and robustness with respect to the aspect ratio is not in general ensured and often unlikely to hold in practice.

In [40, 42], we showed that NN and FETI methods can be successfully devised for the particular geometrically refined boundary layer meshes commonly used for *hp* finite element approximations of two-dimensional problems. Indeed, these meshes are highly anisotropic, but of a particular type:

1. they are obtained by refining an initial *shape-regular* mesh (macromesh);

2. refinement is only carried *towards* the boundary of the computational domain.

These properties, also shared by three-dimensional meshes, allowed us to obtain condition number bounds for the corresponding preconditioned operators that only grow polylogarithmically with the polynomial degree, as is the case of p approximations on shape regular meshes. Our understanding and analysis was confirmed by numerical experiments. In particular, we choose the macromesh

as a decomposition into substructures in such a way that subdomains are shape-regular. Roughly speaking, the reason why such favourable condition numbers are retained lies on the fact that upper bounds come from stable decompositions of finite element functions into components associated to geometrical objects (typically vertices and edges of the subdomains in two dimensions). Because of our particular meshes, only components associated to *internal* vertices need to be considered, i.e., relative to vertices in a neighborhood of which the mesh is shape-regular.

Three-dimensional boundary layer meshes also share the two characteristics mentioned above. However, stable decompositions now involve face and wire-basket components, where the wirebasket is the union of the subdomain edges and vertices that do not lie on the external boundary of the computational domain. By considering, for instance, an edge E of a macroelement that share a face with Ω (see the face patch in Figures 1, left, or 2), decoupling of face and wirebasket components is now also performed close to $\partial\Omega$, and thus where the mesh is not shape-regular. In this work, we are however able to provide condition number bounds that only grow polylogarithmically with the polynomial degree, as in the two-dimensional case, and are independent of arbitrarily large aspect ratios of the mesh.

The core of this work lies in the careful modification and derivation of certain Sobolev type inequalities that are independent of the aspect ratio of the mesh for wirebasket and face components of finite element functions; see section 7. Provided such inequalities are available, the definition of the algorithms and their analysis are fairly standard procedures in DD methods and proceed as in the two-dimensional case in [40]. Here, we will only consider Neumann-Neumann methods, but note that the estimates derived can be employed for the analysis of one-level FETI methods in a straightforward way; see [17, 40].

We limit our analysis to the case of nodal basis functions built on Gauss-Lobatto nodes. In addition, we only consider the model problem (1), which does not have boundary layers but only corner and edge singularities. However, our tensor-product meshes can also be employed when only singularities are present and do not require the use of hanging nodes. We recall that numerical results in [42] for two-dimensional problems showed that better performance is obtained for certain singularly perturbed problems which exhibit boundary layers. In addition, a linear dependence in k for the condition number was observed for problems with geometric refinement towards interfaces that lie in the interior of the computational domain.

The remainder of this paper is organized as follows: in sections 2 and 3, we introduce our continuous and discrete problems, respectively. Geometric boundary layer meshes are introduced in section 4. A particular choice of basis functions is given in section 5 and our Neumann-Neumann preconditioners are defined in section 6. Section 7 is the core of this work and is devoted to the proof of some discrete Sobolev type inequalities. Comparison results for certain discrete harmonic extensions are given in section 8. Condition number bounds

are then proven in section 9. Section 10 contains some numerical results, while some concluding remarks and perspectives are presented in section 11.

2 Problem setting

We consider a linear, elliptic problem on a bounded polyhedral domain $\Omega \subset \mathbb{R}^3$ of unit diameter, formulated variationally as:
Find $u \in H_0^1(\Omega)$, such that

$$a(u,v) = \int_\Omega \rho(\mathbf{x}) \nabla u \cdot \nabla v \, d\mathbf{x} = f(v), \quad v \in H_0^1(\Omega). \tag{1}$$

As usual, $H^1(\Omega)$ is the space of square summable functions with square summable first derivatives, and $H_0^1(\Omega)$ its subspace of functions that vanish on $\partial\Omega$. The functional $f(\cdot)$ belongs to the dual space $H^{-1}(\Omega)$. Here $\mathbf{x} = (x, y, z)$ denotes the position vector.

The coefficient $\rho(\mathbf{x}) > 0$ can be discontinuous, with very different values for different subregions, but we allow it to vary only moderately within each subregion. We will in fact assume that the region is the union of elements (also called subdomains, substructures, or macroelements) $\{\Omega_i\}$. Without decreasing the generality of our results, we will only consider the piecewise constant case:

$$\rho(\mathbf{x}) = \rho_i, \quad \mathbf{x} \in \Omega_i.$$

In the case of a region of diameter H_i, such as the substructure Ω_i, we use a norm with different relative weights obtained by a simple dilation argument:

$$\|u\|_{1,\Omega_i}^2 = |u|_{1,\Omega_i}^2 + \frac{1}{H_i^2} \|u\|_{0,\Omega_i}^2. \tag{2}$$

Here, $\|\cdot\|_{0,\Omega_i}$ and $|\cdot|_{1,\Omega_i}$ denote the norm in $L^2(\Omega_i)$ and the seminorm in $H^1(\Omega_i)$, respectively. In the following we also employ the space $W^{1,\infty}(\Omega_i)$ of bounded functions with bounded derivatives; see, e.g., [27].

3 *hp* finite element approximations

We now specify a particular choice of finite element spaces. Given an affine quadrilateral mesh $\mathcal{T}$ of Ω and a polynomial degree $k \geq 1$, we consider the following finite element spaces:

$$X = X^k(\Omega; \mathcal{T}) := \left\{ u \in H_0^1(\Omega) \,|\quad u_{|_K} \in \mathbb{Q}_k(K),\ K \in \mathcal{T} \right\}. \tag{3}$$

Here $\mathbb{Q}_k(K)$ is the space of polynomials of maximum degree k in each variable on K. In the following, we may drop the reference to k, Ω, and/or $\mathcal{T}$ whenever there is no confusion.

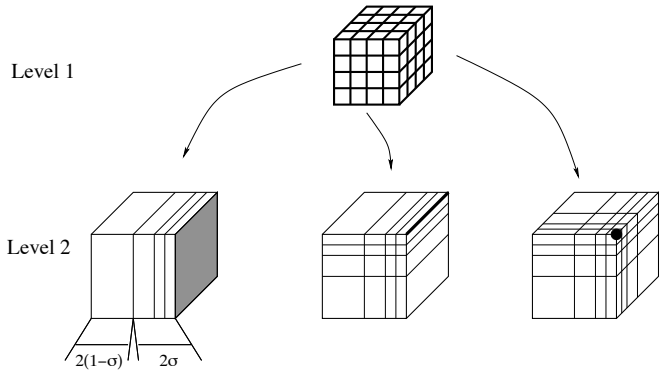

Figure 1: Hierarchic structure of a boundary layer mesh, with $\sigma = 0.5$ and $n = 3$.

In this paper, we always assume that the meshes are *regular*, i.e, the intersection between neighboring elements is either a vertex, or an edge, or a face that is common to the *two* elements.

A finite element approximation of (1) consists of finding $u \in X$, such that

$$a(u, v) = f(v), \quad v \in X. \tag{4}$$

4 Geometric boundary layer meshes

In order to resolve boundary layers and/or singularities, geometrically graded meshes can be employed. They are determined by a mesh grading factor $\sigma \in (0, 1)$ and a refinement level $n \geq 0$. The number of layers is $n + 1$ and the thinnest layer has a width proportional to σ^n. Robust exponential convergence of hp finite element approximations is achieved if n is suitably chosen. For singularity resolution, n is required to be proportional to the polynomial degree k; see [4, 5]. For boundary layers, the width of the thinnest layer needs to be comparable to that of the boundary layer; see [26, 36, 37].

A geometric boundary layer mesh $\mathcal{T} = \mathcal{T}_{bl}^{n,\sigma}$ is, roughly speaking, the tensor product of meshes that are geometrically refined towards the faces. Figure 1 shows the construction of a geometric boundary layer mesh $\mathcal{T}_{bl}^{n,\sigma}$.

The mesh $\mathcal{T}_{bl}^{n,\sigma}$ is built by first considering an initial shape-regular macro-triangulation $\mathcal{T}_m$, possibly consisting of just one element, which is successively refined. This process is illustrated in Figure 1. Every macroelement can be refined isotropically (not shown) or anisotropically in order to obtain so-called face, edge, or corner patches (Figure 1, level 2). Here and in the following, we only consider patches obtained by triangulating the reference cube $\hat{Q} := I^3$, with $I := (-1, 1)$. A patch for an element $K_m \in \mathcal{T}_m$ is obtained by using an

affine mapping $F_{K_m} : \hat{Q} \to K_m$. The stability properties proven for patches on the reference cube are equally valid for an arbitrary shape-regular element $K_m \in \mathcal{T}_m$, with a constant that is independent of the diameter of K_m.

A **face patch** is given by an anisotropic triangulation of the form

$$\mathcal{T}_f := \{K_x \times I \times I \mid \quad K_x \in \mathcal{T}_x\}, \tag{5}$$

where $\mathcal{T}_x$ is a mesh of I, geometrically refined towards, say $x = 1$, with grading factor $\sigma \in (0, 1)$ and n levels of refinement; see Figure 1 (level 2, left). We note that the mesh $\mathcal{T}_x \times \{I\}$ of $\hat{S} := I^2$ is a two-dimensional *edge patch*.

An **edge patch** is given by a triangulation

$$\mathcal{T}_e = \mathcal{T}_e^{bl} := \{K_x \times K_y \times I \mid \quad K_x \in \mathcal{T}_x,\ K_y \in \mathcal{T}_y\} = \{K_{xy} \times I \mid \quad K_{xy} \in \mathcal{T}_{xy}\}, \tag{6}$$

where $\mathcal{T}_x$ and $\mathcal{T}_y$ are meshes of I, geometrically refined towards, say $x = 1$ and $y = 1$, respectively, with grading factor $\sigma \in (0, 1)$ and total number of layers n; see Figure 1 (level 2, center). The mesh $\mathcal{T}_{xy}$ of $\hat{S}$ is a two-dimensional *corner patch*.

In a similar way, we can define a **corner patch** $\mathcal{T}_c$:

$$\mathcal{T}_c = \mathcal{T}_c^{bl} := \{K_x \times K_y \times K_z \mid \quad K_x \in \mathcal{T}_x,\ K_y \in \mathcal{T}_y,\ K_z \in \mathcal{T}_z\},$$

where $\mathcal{T}_x$, $\mathcal{T}_y$, and $\mathcal{T}_z$ are meshes of I, geometrically refined towards, say $x = 1$, $y = 1$, and $z = 1$, respectively; see Figure 1 (level 2, right).

We note that every element $\hat{K}$ of $\mathcal{T}_f$, $\mathcal{T}_e$, and $\mathcal{T}_c$ on the reference cube is of the form $(0, h_x) \times (0, h_y) \times (0, h_z)$ (after a possible translation and rotation) and is thus obtained from the reference element by an affine mapping $F_{\hat{K}} : \hat{Q} \to \hat{K}$ of the form

$$[x \quad y \quad z]^T = [(h_x/2)(\hat{x} + 1) \quad (h_y/2)(\hat{y} + 1) \quad (h_z/2)(\hat{z} + 1)]^T. \tag{7}$$

The aspect ratio of $\hat{K}$ is the maximum of all possible ratios of h_x, h_y, and h_z. Since the macromesh consists of affinely mapped elements K_m, every element K of the global mesh $\mathcal{T} = \mathcal{T}_{bl}^{n,\sigma}$ is obtained from the reference element by combining two affine mappings

$$K = F_K(\hat{Q}) = F_{K_m}(F_{\hat{K}}(\hat{Q})), \quad K \subset K_m \in \mathcal{T}_m. \tag{8}$$

Since $\mathcal{T}_m$ is shape-regular, the aspect ratio is determined only by $F_{\hat{K}}$; cf. (7). Finally we note that the aspect ratio of the mesh is determined by σ and n, and is proportional to σ^{-n}.

As in [40], our analysis will be made for a prototype mesh, obtained from a shape-regular (not necessarily quasi-uniform) macromesh, by refining elements that only touch $\partial\Omega$, either as corner, edge, or face patches. Such meshes only consist of four types of patches: unrefined, face, edge, and corner patches. We also recall that in practical applications σ is bounded away from one and zero.

5 Basis functions on Gauss-Lobatto nodes

For the space $X^k(\Omega;\mathcal{T})$, we choose nodal basis functions on the Gauss-Lobatto nodes. We denote by $GLL(k)$ the set of Gauss-Lobatto points $\{\xi_i;\ 0 \le i \le k\}$ on $I=(-1,1)$ in increasing order and by $\{w_i > 0\}$ the corresponding weights; see [6, Sect. 4]. We recall that the quadrature formula based on $GLL(k)$ has order $2k-1$ and, in addition,

$$\|u\|^2_{0,I} \le \sum_{i=0}^{k} u(\xi_i)^2\, w_i \le 3\,\|u\|^2_{0,I}, \quad u \in \mathbb{Q}_k(I); \tag{9}$$

see [6, Rem. 13.3].

For the reference cube $\hat{Q}=(-1,1)^3$ we set $GLL(k)^3 = \{\xi_{ijl} = (\xi_i,\xi_j,\xi_l);\ 0 \le i,j,l \le k\}$. In the following, we use the same notation for the mapped Gauss-Lobatto nodes and corresponding weights for an affinely mapped element $K \in \mathcal{T}$.

Given the nodes $GLL(k)^3$, our basis functions on $\mathbb{Q}_k(\hat{Q})$ are the tensor product of k-th order Lagrange interpolating polynomials on $GLL(k)$, defined by

$$\hat{l}_i(\xi_j) = \delta_{ij}. \tag{10}$$

On the reference element we can write

$$u(x,y,z) = \sum_{i=0}^{k}\sum_{j=0}^{k}\sum_{l=0}^{k} u(\xi_i,\xi_j,\xi_l)\ \hat{l}_i(x)\hat{l}_j(y)\hat{l}_l(z), \quad u \in \mathbb{Q}_k(\hat{Q}). \tag{11}$$

For a general element in $\mathcal{T}$, basis functions are obtained by mapping those on the reference element. *Interior* local basis functions correspond to GLL nodes inside $\hat{Q}$ (all local indices differ from 0 and k).

Equation (11) defines an interpolation operator I^k on the reference element

$$I^k u(x,y,z) := \sum_{i=0}^{k}\sum_{j=0}^{k}\sum_{l=0}^{k} u(\xi_i,\xi_j,\xi_l)\ \hat{l}_i(x)\hat{l}_j(y)\hat{l}_l(z).$$

The points $GLL(k)^3$ define a triangulation $\mathcal{T}_k = \mathcal{T}_k(\hat{Q})$ of $\hat{Q}$ in a natural way, consisting of k^3 parallelepipeds. Let $Y^h = Y^h(\hat{Q}) = X^1(\hat{Q};\mathcal{T}_k)$ be the space of piecewise trilinear functions on this mesh. We also denote $Y^k = Y^k(\hat{Q}) = \mathbb{Q}_k(\hat{Q})$. The aspect ratio of $\mathcal{T}_k$ is of the order of k; see [10, Pg. 27] for details. In a similar way we can consider a Gauss-Lobatto mesh on an affinely mapped element K by simply mapping the GLL mesh on $\hat{Q}$. In the following, we will use the notations $\mathcal{T}_k = \mathcal{T}_k(K)$, $Y^h = Y^h(K)$, and $Y^k = Y^k(K)$, to denote the GLL mesh, the piecewise trilinear finite element space, and $\mathbb{Q}_k$, respectively, for a mapped element. If the aspect ratio of K is, e.g., h_x/h_y (cf. (7) and (8)), then that of the corresponding $\mathcal{T}_k$ is $(h_x/h_y)k$.

There is a one-to-one correspondence between Y^h and Y^k given by

$$I^k : Y^h \to Y^k, \quad I^h : Y^k \to Y^h,$$

where I^h is the nodal interpolation operator on Y^h. We use the notation $u_h \in Y^h$ and $u_k \in Y^k$ in order to denote two corresponding functions.

Lemma 5.1 *Let $\hat{K} = (0, h_x) \times (0, h_y) \times (0, h_z)$. Then there exist positive constants c and C, such that, for $u_h \in Y^h(\hat{K})$,*

$$c\|u_h\|_{0,\hat{K}} \le \|u_k\|_{0,\hat{K}} \le C\|u_h\|_{0,\hat{K}},$$
$$c\|\partial_x(u_h)\|_{0,\hat{K}} \le \|\partial_x(u_k)\|_{0,\hat{K}} \le C\|\partial_x(u_h)\|_{0,\hat{K}},$$

with, in particular, c and C independent of h_x, h_y, h_z, and k. Similar bounds hold for the y and z derivatives. If $K \in \mathcal{T}$ is given by (8), then, for $u_h \in Y^h(K)$,

$$c\|u_h\|_{0,K} \le \|u_k\|_{0,K} \le C\|u_h\|_{0,K},$$
$$c|u_h|_{1,K} \le |u_k|_{1,K} \le C|u_h|_{1,K}$$

where the constants are independent of the diameter and the aspect ratio of K, and k.

The proof of the above result can be found in [9, Sect. 2] for $K = \hat{Q}$. For an affinely mapped element a scaling argument can be used. We note that thanks to Lemma 5.1 we can equivalently work with functions in Y^k or Y^h.

The following result can be found in [10, Lem. 3.3.3].

Lemma 5.2 *Let $\hat{K} = (0, h_x) \times (0, h_y) \times (0, h_z)$ and $u_h \in Y^h(\hat{K})$. Given $\theta \in W^{1,\infty}(\hat{K})$, with*

$$\|\theta\|_{\infty,\hat{K}} \le C, \quad \|\nabla\theta\|_{\infty,\hat{K}} \le C/r,$$

then

$$\|I^h(\theta u_h)\|^2_{0,\hat{K}} \le C\|u_h\|^2_{0,\hat{K}},$$
$$\|\partial_x I^h(\theta u_h)\|^2_{0,\hat{K}} \le C(|u_h|^2_{1,\hat{K}} + r^{-2}\|u_h\|^2_{0,\hat{K}}),$$

where C is independent of h_x, h_y, h_z, and k. Similar bounds hold for the y and z derivatives. If $K \in \mathcal{T}$ is given by (8), then, for $u_h \in Y^h(K)$,

$$\|I^h(\theta u_h)\|^2_{0,K} \le C\|u_h\|^2_{0,K},$$
$$|I^h(\theta u_h)|^2_{1,K} \le C(|u_h|^2_{1,K} + r^{-2}\|u_h\|^2_{0,K}),$$

where C is independent of the diameter and the aspect ratio of K, and k.

Given an element $\hat{K} = (0, h_x) \times (0, h_y) \times (0, h_z)$ and a coordinate direction, say x, , let a, b, c, and d be the vertices of a face of $\hat{K}$ perpendicular to this direction, and let a', b', c', and d' be the corresponding points on the parallel face. The following lemma relies on trivial properties of trilinear functions; cf. [10, Lem. 3.3.1].

Lemma 5.3 *Let $\hat{K} = (0, h_x) \times (0, h_y) \times (0, h_z)$ and a, b, c, and d be the vertices of a face of $\hat{K}$ perpendicular to the x direction. Then there are constants independent of h_x, h_y, and h_z, such that, if u is trilinear on $\hat{K}$,*

$$c\|u\|^2_{0,\hat{K}} \le h_x h_y h_z \sum_{\mathbf{x}=a,b,c,d} (u(\mathbf{x})^2 + u(\mathbf{x}')^2) \le C\|u\|^2_{0,\hat{K}},$$
$$c\|\partial_x u\|^2_{0,\hat{K}} \le (h_x h_y h_z / h_x^2) \sum_{\mathbf{x}=a,b,c,d} (u(\mathbf{x}) - u(\mathbf{x}'))^2 \le C\|\partial_x u\|^2_{0,\hat{K}},$$
$$c\|\partial_x u\|^2_{\infty,\hat{K}} \le h_x^{-2} \sum_{\mathbf{x}=a,b,c,d} (u(\mathbf{x}) - u(\mathbf{x}'))^2 \le C\|\partial_x u\|^2_{\infty,\hat{K}}.$$

Similar bounds hold for the y and z derivatives.

6 Neumann-Neumann methods

Iterative substructuring methods rely on a non-overlapping partition into substructures. We mention [39, Ch. 4] as a general reference to this section. In our algorithms the substructures are chosen as the macroelements in $\mathcal{T}_m = \{\Omega_i \mid 1 \le i \le N\}$. We recall that the macroelements are shape-regular. This appears to be essential for the analysis and good performance.

We define the boundaries $\Gamma_i = \partial\Omega_i \setminus \partial\Omega$ and the interface Γ as their union. We remark that Γ is the union of the interior subdomain *faces*, regarded as open sets, which are shared by two subregions, and subdomain *edges* and *vertices*, which are shared by more than two subregions. Vertices can only be endpoints of edges. In the following, we tacitly assume that points on $\partial\Omega$ are excluded from the geometrical objects that we consider, or, in other words, we will only deal with geometrical objects (faces, edges, vertices, ...) that belong to Γ. We denote the faces of Ω_i by F^{ij}, its edges by E^{ij}, its vertices by V^{ij}, and its *wirebasket*, defined as the union of its edges and vertices, by W^i. Occasionally, we will also use faces, edges, and vertices with one or no superscript. If a vertex (edge) lies on $\partial\Omega$ we will regard it as part of the internal edge (resp., face) that shares it with $\partial\Omega$.

When restricted to the subdomain Ω_i, the global triangulation $\mathcal{T}$ determines a local mesh $\mathcal{T}_i$. This mesh can be of four types: face, edge, corner, or consisting of just one element. We define the local spaces $X_i = X^k(\Omega_i; \mathcal{T}_i)$, of local finite element functions that vanish on $\partial\Omega \cap \partial\Omega_i$

In our analysis, we will also employ the GLL mesh $\mathcal{T}_k(\Omega_i)$ on Ω_i, generated by the local GLL meshes $\mathcal{T}_k(K)$ for $K \in \mathcal{T}_i$. The corresponding space of piecewise trilinear functions on $\mathcal{T}_k(\Omega_i)$ that vanish on $\partial\Omega \cap \partial\Omega_i$ is denoted by $Y^h(\Omega_i)$. We set $Y^k(\Omega_i) = X^k(\Omega_i; \mathcal{T}_i)$.

We next define the local bilinear forms

$$a_i(u, v) = \int_{\Omega_i} \rho_i \nabla u \cdot \nabla v \, d\mathbf{x}, \quad u, v \in X_i.$$

We note that if Ω_i is a *floating* subdomain (i.e., its boundary does not touch $\partial\Omega$), $a_i(\cdot,\cdot)$ is only positive semi-definite and for $u \in X_i$ we have

$$a_i(u,u) = 0 \quad \text{iff} \quad u \text{ constant in } \Omega_i.$$

The sets of nodal points on Γ_i, Γ, F^{ij}, E^{ij}, and W^i are denoted by $\Gamma_{i,h}$, Γ_h, F_h^{ij}, E_h^{ij}, and W_h^i, respectively. We will identify these sets with the corresponding sets of degrees of freedom. As for the corresponding regions, we will also use notations with one or no superscript.

We introduce some spaces defined on the interfaces: U_i is the space of restrictions to Γ_i of functions in $X^k(\Omega_i;\mathcal{T}_i)$ and U of restrictions to Γ of functions in $X^k(\Omega;\mathcal{T})$. We note that functions in U_i and U are uniquely determined by the nodal values in $\Gamma_{i,h}$ and Γ_h, respectively. For every substructure Ω_i, there is a natural interpolation operator

$$R_i^T : U_i \longrightarrow U,$$

that extends a function on Γ_i to a global function on Γ with vanishing degrees of freedom in $\Gamma_h \setminus \Gamma_{i,h}$. Its transpose with respect to the Euclidean scalar product $R_i : U \to U_i$ extracts the degrees of freedom in $\Gamma_{i,h}$.

Once a vector $u \in X^k(\Omega;\mathcal{T})$ is expanded using the basis functions introduced in section 5, Problem (4) can be written as a linear system

$$Au = f.$$

We recall that the condition number of A is expected to grow at least as $k^3/(h_{min})^2 \sim k^3\sigma^{-2n} \sim k^3\sigma^{-2k}$ (see [25] for a result in two dimensions) and may thus be extremely large for large values of k.

The contributions to the stiffness matrix and the right hand side can be formed one subdomain at a time. The stiffness matrix is then obtained by *subassembly* of these parts. We will order the nodal points interior to the subdomains first, followed by those on the interface Γ. Similarly, for the stiffness matrix relative to a substructure Ω_i, we have

$$A^{(i)} = \begin{pmatrix} A_{II}^{(i)} & A_{I\Gamma}^{(i)} \\ A_{\Gamma I}^{(i)} & A_{\Gamma\Gamma}^{(i)} \end{pmatrix}.$$

In a first step of many iterative substructuring algorithms, the unknowns in the interior of the subdomains are eliminated by block gaussian elimination. In this step, the Schur complements, with respect to the variables associated with the boundaries of the individual substructures, are calculated. The resulting linear system can be written as

$$Su_\Gamma = g_\Gamma. \tag{12}$$

Given the local Schur complements

$$S_i = A_{\Gamma\Gamma}^{(i)} - A_{I\Gamma}^{(i)^T} A_{II}^{(i)^{-1}} A_{I\Gamma}^{(i)} : U_i \longrightarrow U_i,$$

we have

$$S = \sum_{i=1}^{N} R_i^T S_i R_i : U \longrightarrow U$$

and an analogous formula can be found for g_Γ; see [39, Ch. 4].

A function $u^{(i)}$ defined on Ω_i is said to be discrete harmonic on Ω_i if

$$A_{II}^{(i)} u_I^{(i)} + A_{I\Gamma}^{(i)} u_\Gamma^{(i)} = 0.$$

In this case, it is easy to see that $\mathcal{H}_i(u_\Gamma^{(i)}) := u^{(i)}$ is completely defined by its value on Γ_i. The space of piecewise discrete harmonic functions u consists of functions in X that are discrete harmonic on each substructure. In this case, $u =: \mathcal{H}(u_\Gamma)$ is completely defined by its value on Γ.

Our preconditioners will be defined with respect to the inner product

$$s(u, v) = u^T S v, \quad u, v \in U.$$

It follows immediately from the definition of S that $s(\cdot, \cdot)$ is symmetric and coercive.

The following lemma results from elementary variational arguments.

Lemma 6.1 *Let $u_\Gamma^{(i)}$ be the restriction of a finite element function to Γ_i. Then the discrete harmonic extension $u^{(i)} = \mathcal{H}_i(u_\Gamma^{(i)})$ of $u_\Gamma^{(i)}$ into Ω_i satisfies*

$$a_i(u^{(i)}, u^{(i)}) = \min_{v^{(i)}|_{\partial\Omega_i} = u_\Gamma^{(i)}} a_i(v^{(i)}, v^{(i)}) = u_\Gamma^{(i)^T} S^{(i)} u_\Gamma^{(i)}.$$

Analogously, if u_Γ is the restriction of a finite element function to Γ, the piecewise discrete harmonic extension $u = \mathcal{H}(u_\Gamma)$ of u_Γ into the interior of the subdomains satisfies

$$a(u, u) = \min_{v|_\Gamma = u_\Gamma} a(v, v) = s(u, u) = u_\Gamma^T S u_\Gamma.$$

This lemma ensures that instead of working with functions defined on the interface Γ, we can equivalently work with the corresponding discrete harmonic extensions. For this reason, in the following we will identify spaces of traces on the interfaces, U_i and U, with spaces of discrete harmonic extensions. We point out however that due to the particular meshes considered, we cannot equivalently work with norms of local discrete harmonic extensions and traces on the subdomain boundaries since our local meshes are not in general quasi-uniform or shape-regular, and stable discrete harmonic extensions cannot be found in general.

Neumann-Neumann methods provide preconditioners for the Schur complement system: instead of solving (12) using, e.g., the conjugate gradient method, they employ an equivalent system involving a preconditioned operator of the form

$$\hat{S}^{-1}S = P_{NN} = P_0 + (I - P_0)(\sum_{i=1}^{N} P_i)(I - P_0).$$

We refer to [12, 24, 30, 17] for some NN methods for the h and p finite element approximations. We are unaware on any such method for hp approximations.

The operators P_i are projection-like operators associated to a family of subspaces U_i and determined by a set of local bilinear forms defined on them

$$\tilde{s}_i(u, v), \quad u, v \in U_i.$$

Given the interpolation operators $R_i^T : U_i \to U$, we have

$$P_i = R_i^T \tilde{P}_i, \quad \tilde{P}_i : U \longrightarrow U_i, \tag{13}$$

with

$$\tilde{s}_i(\tilde{P}_i u, v_i) = s(u, R_i^T v_i), \quad v_i \in U_i. \tag{14}$$

While P_0 is associated to a low-dimensional global problem, the others are associated to the single substructures. The remainder of this section is devoted to the definition of the various components of P_{NN}.

An important role is played by a family of weighted counting functions δ_i, which are associated with and defined on the individual Γ_i (cf. [11, 12, 24, 35, 30]) and are defined for $\gamma \in [1/2, \infty)$. Given Ω_i and $\mathbf{x} \in \Gamma_{i,h}$, $\delta_i(\mathbf{x})$ is determined by a sum of contributions from Ω_i and its relevant next neighbors,

$$\delta_i(\mathbf{x}) = \sum_{j \in \mathcal{N}_\mathbf{x}} \rho_j^\gamma(\mathbf{x}) / \rho_i^\gamma(\mathbf{x}), \quad \mathbf{x} \in \Gamma_{i,h}. \tag{15}$$

Here $\mathcal{N}_\mathbf{x}$, $\mathbf{x} \in \Gamma_h$, is the set of indices j of the subregions such that $\mathbf{x} \in \Gamma_{j,h}$. The function δ_i is discrete harmonic and thus belongs to U_i. The pseudoinverses $\delta_i^\dagger \in U_i$ are defined, for $\mathbf{x} \in \Gamma_{i,h}$, by

$$\delta_i^\dagger(\mathbf{x}) = \delta_i^{-1}(\mathbf{x}), \quad \mathbf{x} \in \Gamma_{i,h}. \tag{16}$$

We note that these functions provide a partition of unity:

$$\sum_{i=1}^{N} R_i^T {\delta_i}^\dagger(\mathbf{x}) \equiv 1. \tag{17}$$

In particular, for $u \in U$ we can use the formula

$$u = \sum_{i=1}^{N} R_i^T u_i, \quad \text{with } u_i = \mathcal{H}_i(\delta_i^\dagger u). \tag{18}$$

Here and from now on, we will tacitly assume that whenever we write $\mathcal{H}_i(uv)$ or $\mathcal{H}(uv)$ we first form $I^k(uv)$, i.e., map the product of the two functions u and v into the hp finite element space by interpolation, and then extend the result as a discrete harmonic function. If there is no confusion, we will sometime use the notation uv in order to denote $I^k(uv)$ or $\mathcal{H}_i(uv)$.

A coarse space U_0 of minimal dimension is defined as

$$U_0 = \text{span}\{R_i^T \delta_i^\dagger\} \subset U,$$

where the span is taken over the floating subdomains. We note that U_0 consists of piecewise discrete harmonic functions and R_0^T is the natural injection $U_0 \subset U$. We consider an exact solver on U_0

$$\tilde{s}_0(u,v) := a(\mathcal{H}u, \mathcal{H}v) = a(u,v).$$

For every substructure Ω_i, the local bilinear form is

$$\tilde{s}_i(u,v) := a_i(\mathcal{H}_i(\delta_i u), \mathcal{H}_i(\delta_i v)), \quad u, v \in U_i.$$

For a floating subdomain $\tilde{P}_i$ is defined only for those $u \in U$ for which $s(u,v) = 0$ for all $v = R_i^T v_i$ such that $\mathcal{H}_i(\delta_i v_i)$ is constant on Ω_i. This condition is satisfied if $a(u, R_i^T \delta_i^\dagger) = 0$; we note that $R_i^T \delta_i^\dagger$ is a basis function for U_0. For such subdomains, we make the solution $\tilde{P}_i u$ of (14) unique by imposing the constraint

$$\int_{\Omega_i} \mathcal{H}_i(\delta_i \tilde{P}_i u) d\mathbf{x} = 0, \tag{19}$$

which just means that we select the solution orthogonal to the null space of the Neumann operator. Thus, $Range(\tilde{P}_i)$ has codimension 1 with respect to the space U_i.

We can equally well use matrix notations. Let D_i be the diagonal matrix with the elements $\delta_i^\dagger(\mathbf{x})$ corresponding to the point $\mathbf{x} \in \Gamma_{i,h}$. Then

$$\tilde{s}_i(u,v) = u^T D_i^{-1} S_i D_i^{-1} v.$$

We also have,

$$P_i = R_i^T D_i S_i^\dagger D_i R_i S,$$

where $S_i^\dagger$ is a pseudoinverse of S_i. Analogously for the coarse projection

$$P_0 = R_0^T S_0^{-1} R_0 S,$$

where $S_0 = R_0 S R_0^T$ the restriction of S to U_0

The main result of this paper is a bound for the condition number of P_{NN}. Such bound can be found using the abstract Schwarz theory; see, e.g., [39, Ch. 6]. We refer to [24, 12, 30, 39, 17] for similar proofs.

A uniform bound for the smallest eigenvalue can be found using the decomposition (18) and the fact that P_0 is an orthogonal projection.

Lemma 6.2 *We have*

$$s(P_{NN}u, u) \geq s(u, u), \quad u \in U.$$

In order to find a bound for the largest eigenvalue, we need a stability property for the local bilinear forms; see, e.g., [39].

Assumption 6.1 *We have*

$$s(R_i^T u_i, R_i^T u_i) \leq \omega\, \tilde{s}_i(u_i, u_i), \qquad u_i \in Range(\tilde{P}_i), \quad i = 1, \cdots, N,$$

with

$$\omega = C\,(1-\sigma)^{-6}\,\left(1 + \log\left(\frac{k}{1-\sigma}\right)\right)^2$$

and C independent of k, n, σ, γ, the coefficients ρ_i, and the diameters H_i.

The proof of Assumption 6.1 is given in section 9. Assumption 6.1 and a coloring argument provide a bound for the largest eigenvalue; see, e.g., [30, Sect. 8].

Lemma 6.3 *Let Assumption 6.1 be satisfied. Then*

$$s(P_{NN}u, u) \leq C\omega s(u, u), \quad u \in U.$$

Consequently the condition number of P_{NN} satisfies

$$\kappa(P_{NN}) \leq C\omega = C\,(1-\sigma)^{-6}\,\left(1 + \log\left(\frac{k}{1-\sigma}\right)\right)^2.$$

7 Decomposition results

A key ingredient for the proof of Assumption 6.1 and for the analysis of many iterative substructuring methods in three dimensions is a decomposition result for local functions in U_i into face and wirebasket components:

$$u = \sum_j u_{F^{ij}} + u_{W^i}, \quad u \in U_i. \tag{20}$$

The face component $u_{F^{ij}}$ vanishes on $\partial\Omega_i \setminus F^{ij}$ and is discrete harmonic. It is uniquely determined by the nodal values in F_h^{ij}. The wirebasket component u_{W^i} is also discrete harmonic and vanishes at all points of $\Gamma_{i,h}$ except at those in W_h^i.

We can further decompose a local functions by also defining edge and vertex components:

$$u = \sum_j u_{F^{ij}} + \sum_j u_{E^{ij}} + \sum_j u_{V^{ij}}, \quad u \in U_i, \tag{21}$$

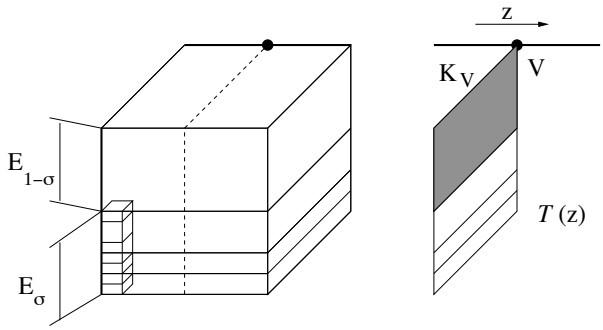

Figure 2: Face patch: partition of an edge E that touches $\partial\Omega$ into $E_{1-\sigma}$ and E_σ (left) and two-dimensional mesh $\mathcal{T}(z)$ for a section corresponding to a constant z (right).

where $u_{E^{ij}}$ is discrete harmonic and vanishes on $\partial\Omega_i \setminus E^{ij}$, and $u_{V^{ij}}$ vanishes at all nodes in $\Gamma_{i,h}$ except at the vertex V^{ij}. We recall that we exclude geometrical objects on $\partial\Omega$ and that therefore the sums in (20) and (21) are taken over faces, edges, and vertices that do not belong to $\partial\Omega$. Discrete harmonic functions of type $u_{F^{ij}}$, $u_{E^{ij}}$, $u_{V^{ij}}$, and u_{W^i} are called face, edge, vertex, and wirebasket functions, respectively.

Here and in the following section, we only carry out proofs for the reference cube $\hat{Q}$: since elements in the macromesh $\mathcal{T}_m$ are shape-regular and affinely mapped, the corresponding bounds for a generic substructure $\Omega_i \in \mathcal{T}_m$, of diameter H_i, can be obtained by a standard scaling argument and involve the scaled norm (2). We recall that we only need to consider four types of patches: face, edge, corner, and unrefined ones, together with the corresponding triangulations $\mathcal{T}_f$, $\mathcal{T}_e$, $\mathcal{T}_c$, and $\hat{Q}$, respectively; cf. Figures 1. We recall that a generic patch is denoted by Ω_i and its triangulation by $\mathcal{T}_i$.

7.1 Wirebasket components

Given an edge $E = E^{ij} \subset W^i$, we define a discrete L^2 norm on E. If E does not touch the boundary $\partial\Omega$, we simply set

$$\|u\|_{h,E} := \|u\|_{0,E}.$$

Let now E be an edge that touches $\partial\Omega$; see Figure 2, left, for an example of a face patch. After a possible translation and rotation, E can always be written as

$$E = \{(1, 1, z) \,|\, z \in I\}.$$

Then, the local mesh $\mathcal{T}_i$ gives rise to a one-dimensional triangulation on E, $\mathcal{T}_E$, which is not quasiuniform and is geometrically refined towards one end point,

say $z = 1$. In addition, E can be partitioned as

$$\overline{E} = \overline{E}_{1-\sigma} \cup \overline{E}_{\sigma}, \qquad E_{1-\sigma} = (-1, -1 + 2(1-\sigma)), \quad E_{\sigma} = (-1 + 2(1-\sigma), 1).$$

We note that $E_{1-\sigma}$ consists of exactly one element of length $2(1-\sigma)$ in $\mathcal{T}_E$, while the elements on E_σ are geometrically refined towards $z = 1$. We now consider the GLL mesh $\mathcal{T}_k(\Omega_i)$ and observe that all the elements that touch the edge E have the same diameters $h_{i,x}$ and $h_{i,y}$, along the two directions perpendicular to E; cf. Figure 2. Indeed, $h_{i,x}$ and $h_{i,y}$ are of order k^{-2}, for a face patch, of order $k^{-2}(1-\sigma)$, for a corner patch, and of order k^{-2} and $k^{-2}(1-\sigma)$, respectively, for an edge patch. Moreover, thanks to our particular meshes and to the fact that local spaces of the same degree k are employed on each element, we have the following property:

Property 7.1 *Let E be an edge parallel to, e.g., z, that is shared by two substructures Ω_i and Ω_j. Then, the meshsizes $h_{i,x}$ and $h_{j,x}$, and $h_{i,y}$ and $h_{j,y}$ are comparable. In particular, there exist constants, depending only on the aspect ratios of Ω_i and Ω_j, such that*

$$c(1-\sigma)h_{i,x} \leq h_{j,x} \leq C(1-\sigma)^{-1}h_{i,x}.$$

Similar bounds hold for $h_{i,y}$ and $h_{j,y}$.

We define

$$\|u\|^2_{h,E} := \|u\|^2_{0,E} + \|u\|^2_{h,E_\sigma} = \|u\|^2_{0,E} + h_{i,x}h_{i,y}\|\partial_z u\|^2_{0,E_\sigma}.$$

We note that in this case the discrete norm is obtained by adding to the L^2 norm on E a weighted L^2 norm of $\partial_z u$ over a part of E where $\mathcal{T}_E$ is not quasiuniform. A discrete wirebasket norm is obtained by summing the contributions over all the edges:

$$\|u\|^2_{h,W^i} := \sum_{E \subset W^i} \|u\|^2_{h,E}$$

Lemma 7.1 *Let $u_{W^i} \in U_i$ be discrete harmonic and vanish at all nodal points $\Gamma_{i,h}$ except at those on W^i. Then there is a constant independent of u_{W^i}, H_i, σ, and n, such that*

$$|u_{W^i}|^2_{1,\Omega_i} \leq C(1-\sigma)^{-2}\|u_{W^i}\|^2_{h,W^i}.$$

Proof. The result follows by estimating the energy norm of the zero extension of the boundary values and by noting that the harmonic extension has a smaller energy (cf. Lemma 6.1). More precisely, let u_k be the function that vanishes at all nodal points in $\Omega_{i,h} \cup \Gamma_{i,h}$ except at those on W^i and $u = u_h = I^h u_k$ the corresponding piecewise trilinear function defined on the GLL mesh $\mathcal{T}_k(\Omega_i)$. We will estimate the energy of u_h on each element $K \in \mathcal{T}_k(\Omega_i)$ that touch an edge

$E \subset W^i$. Without loss of generality, we assume that E is parallel to the z axis. We only consider the worst possible case, i.e., that of a face patch and refer to Figure 2.

Let us first suppose that E does not touch $\partial\Omega$. For a face patch, K has dimensions h_x, h_y, and h_z of order

$$\begin{array}{l} k^{-2} \times k^{-2}(1-\sigma) \times k^{-2}, \quad \text{or} \\ k^{-2} \times k^{-2}(1-\sigma) \times k^{-1}, \end{array}$$

and thus

$$\begin{array}{l} c(1-\sigma)h_x \le h_y \le Ch_x, \\ h_x \le Ch_z; \end{array} \tag{22}$$

see Figure 2. If a and b are the vertices of K that lie on E, Lemma 5.3 yields

$$\|\partial_x u\|^2_{0,K} \le C(h_y h_z/h_x)\,(u(a)^2 + u(b)^2) \le C\int_a^b u^2 dz,$$

where for the last inequality we have used (22) and standard properties of linear functions. In a similar way, we find

$$\|\partial_y u\|^2_{0,K} \le C(1-\sigma)^{-1}\int_a^b u^2 dz, \qquad \|\partial_z u\|^2_{0,K} \le C\int_a^b u^2 dz.$$

Let now E be an edge that touches $\partial\Omega$ and $K \in \mathcal{T}_k(\Omega_i)$ be an element that shares an edge with $E_{1-\sigma}$. For a face patch, K has dimensions of the order

$$\begin{array}{l} k^{-2} \times k^{-2} \times k^{-2}(1-\sigma), \quad \text{or} \\ k^{-2} \times k^{-2} \times k^{-1}(1-\sigma), \end{array}$$

and thus

$$\begin{array}{l} ch_x \le h_y \le Ch_x, \\ h_x \le C(1-\sigma)^{-1}h_z; \end{array} \tag{23}$$

see Figure 2, left. As before, Lemma 5.3 yields

$$\|\partial_x u\|^2_{0,K} \le C\int_a^b u^2 dz, \quad \|\partial_y u\|^2_{0,K} \le C\int_a^b u^2 dz, \quad \|\partial_z u\|^2_{0,K} \le C(1-\sigma)^{-2}\int_a^b u^2 dz.$$

We are now left with the case of an element $K \in \mathcal{T}_k(\Omega_i)$ that shares an edge with E_σ. We note that the first of (23) remains valid in this case. We then have

$$\|\partial_x u\|^2_{0,K} \le C\int_a^b u^2 dz, \qquad \|\partial_y u\|^2_{0,K} \le C\int_a^b u^2 dz.$$

For $\partial_z u$, we trivially have

$$\|\partial_z u\|^2_{0,K} \le C(h_x h_y/h_z)(u(a)-u(b))^2 \le Ch_x h_y \int_a^b (\partial_z u)^2 dz.$$

The proof is concluded by summing over the elements $K \in \mathcal{T}_k(\Omega_i)$ and using Lemma 5.1. □

We now have a bound for the wirebasket component.

Theorem 7.1 *Let $u \in U_i$ and u_{W^i} be its wirebasket component. Then there is a constant independent of u, H_i, σ, and n, such that*

$$|u_{W^i}|^2_{1,\Omega_i} \leq C(1-\sigma)^{-2}\|u\|^2_{h,W^i}.$$

A complementary result is given by the trace estimates in Lemma 7.2. We first introduce some additional notations. Let E be an edge of a substructure Ω_i. Without loss of generality, we assume that Ω_i coincides with the reference cube $\hat{Q}$ and that $E = \{(1,1,z) \mid z \in I\}$. The intersection between the plane corresponding to a constant $z \in I$ and $\hat{Q}$ is the unit square $\hat{S} = (-1,1)^2$, and the local mesh $\mathcal{T}_i$ gives rise to a two-dimensional mesh $\mathcal{T}(z)$ on $\hat{S}$ which is either a two-dimensional edge or corner patch, or it consists of a single element $\hat{S}$; see Figure 2, right. Let $V = (1,1)$ be the intersection between E and the closure of $\hat{S}$. If $K_V \in \mathcal{T}(z)$ is the two-dimensional element that contains V, we note that, since E does not belong to $\partial\Omega$, K_V has dimensions in $\{2, 2(1-\sigma)\}$, and thus independent of the level of refinement n. For a fixed $(x,y) \in \overline{K_V}$, we finally define the edge $E(x,y) = \{(x,y,z) \mid z \in I\}$.

Lemma 7.2 *Let $u_k \in X_i$ and E and edge of Ω_i. Then there is a constant independent of u_k, H_i, σ, and n, such that*

$$\begin{aligned} \|u_k\|^2_{0,E} &\leq C\,(1-\sigma)^{-2}\,(1+\log k)\,\|u_k\|^2_{1,\Omega_i}, \\ \|u_k\|^2_{h,E} &\leq C\,(1-\sigma)^{-2}\,(1+\log k)\,\|u_k\|^2_{1,\Omega_i}. \end{aligned}$$

Proof. As before, it is enough to find bounds for $u = I^h u_k$. Without loss of generality, we assume $E = \{(1,1,z) \mid z \in I\}$. We consider the two-dimensional mesh $\mathcal{T}(z)$ on the intersection between the plane corresponding to a constant z and the substructure; cf. Figure 2, right. Since geometric refinement on $\mathcal{T}(z)$ takes place far from the vertex $(1,1)$, we can apply the two-dimensional result in [40, Lem. 7.6] and write

$$|u(1,1,z)|^2 \leq C\,(1-\sigma)^{-2}\,(1+\log k)\,\|u(\cdot,\cdot,z)\|^2_{1,\hat{S}}, \quad z \in (-1,1),$$

with a constant that is independent of n, σ, and z. Integrating over z then gives

$$\|u\|^2_{0,E} \leq C\,(1-\sigma)^{-2}\,(1+\log k)\,\|u\|^2_{1,\Omega_i},$$

which proves the first inequality and the second one for edges that do not touch $\partial\Omega$.

We now bound $\|u\|_{h,E_\sigma}$ for an edge that touches the boundary $\partial\Omega$. We consider the one-dimensional GLL meshes for each one of the elements in $\mathcal{T}_E$ and estimate the single contributions from the elements of these meshes. Let e

be one of these elements of length h_z and end points a and b. The edge e belongs to a parallelepiped $K_e \in \mathcal{T}_k(\Omega_i)$. We note that K_e has dimensions $h_x = h_{i,x}$, $h_y = h_{i,y}$, and h_z. Since u is linear on e and trilinear on K_e, we have

$$h_x h_y \int_e \partial_z u^2 dz \leq C \frac{h_x h_y}{h_z} (u(a) - u(b))^2 \leq C \|\partial_z u\|^2_{0,K_e},$$

where, for the last inequality, we have used Lemma 5.3. Summing over the edges e in E_σ yields

$$\|u\|^2_{h,E_\sigma} \leq C \|\partial_z u\|^2_{0,\Omega_i},$$

which, combined with the first inequality, proves the second bound. □

The next lemma can be proved using the two-dimensional bound in [40, Lem. 7.6] and similar arguments as before. We note that it is only valid for edges $E(x,y)$ that are not too far from E and thus not too close to the part of Ω_i where anisotropic refinement takes place.

Lemma 7.3 *Let E be an edge of a substructure Ω_i which is parallel, say, to z and intersects the plane corresponding to a constant z in V. Let in addition K_V be the element in the two-dimensional mesh $\mathcal{T}(z)$ that contains V. Then, for every $(x,y) \in \overline{K}_V$ and $u_k \in X_i$,*

$$\|u_k\|^2_{0,E(x,y)} \leq C\,(1-\sigma)^{-2}\,(1+\log k)\,\|u_k\|^2_{1,\Omega_i}, \tag{24}$$

where C is independent of u_k, σ, n, k, and (x,y), but depends only on the aspect ratio of Ω_i.

Proof. The proof can be carried out as in the previous lemma by using the two-dimensional result in [40, Lem. 7.6]. Indeed, since the point (x,y) belongs to $\overline{K}_V$ and is thus far from the region where anisotropic refinement takes place, we have

$$|u(x,y,z)|^2 \leq C\,(1-\sigma)^{-2}\,(1+\log k)\,\|u(\cdot,\cdot,z)\|^2_{1,\hat{S}}, \quad z \in (-1,1).$$

Integration along z concludes the proof. □

We end this section with a stability result for vertex and edge components. It is a direct consequence of (9) and of the fact that for a vertex function the modified norm $\|\cdot\|_{h,E}$ coincides with $\|\cdot\|_{0,E}$.

Lemma 7.4 *Let E be an edge of a substructure Ω_i and V one of its end points. Then, for every $u \in X_i$,*

$$\|u_V\|^2_{h,W^i} \leq C\|u\|^2_{h,W^i}, \quad \|u_E\|^2_{h,W^i} \leq C\|u\|^2_{h,W^i}, \tag{25}$$

where C is independent of u, σ, n, k.

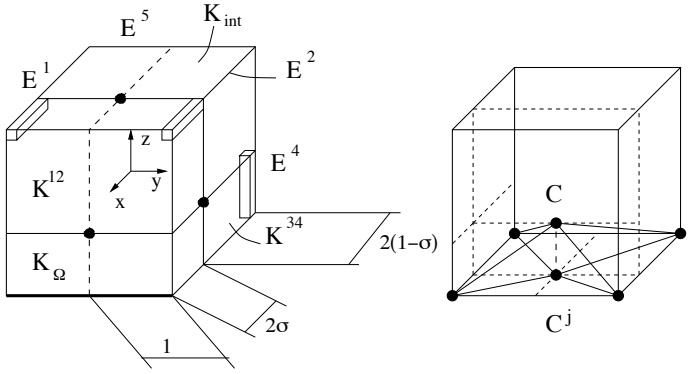

Figure 3: Edge patch on the reference cube $(-1,1)^3$ employed in the proofs of Lemmas 7.5 and 7.6

.

7.2 Face components

We next consider the face contributions of the decomposition (20). Bounds for face contributions on the unrefined patch follow from standard results for spectral elements. For face, edge, and corner patches, we employ cut-off functions θ_F for each face and Lemma 5.2. We note that we need to consider one possible case for faces of the corner patch, and two for the edge and face patches; cf. Figure 1. In this section we only consider the case of an edge patch Ω_i in full detail, with the edge $(1, y, -1)$, $y \in I$, and the two adjacent faces in common with $\partial\Omega$; see Figure 3. The other patches can be dealt with in a similar way.

As shown if Figure 3 for the reference cube, the edges that do not lie on $\partial\Omega$ are denoted by E^l, $l = 1, \ldots, 5$, with E^5 the edge that does not touch the boundary $\partial\Omega$. An edge patch is further partitioned into three regions. The first step of geometric refinement partitions $\hat{Q}$ into four parallelepipeds with dimensions in $\{2, 2(1-\sigma), 2\sigma\}$. Let K_Ω be the one that contains the boundary edge and K_{int} the one that does not touch $\partial\Omega$ and contains the inner edge E^5. The two remaining parallelepipeds are denoted by K^{12} and K^{34} and they touch the edges E^1 and E^2, and E^3 and E^4, respectively. The region K_{edge} is the union of K^{12} and K^{34}; cf. Figure 3.

The proof of the following lemma is a modification of those of [10, Lem. 3.3.6] and [40, Lem. 7.7].

Lemma 7.5 *Given a face F^j of Ω_i that does not lie on $\partial\Omega$, there exists a continuous function θ_{F^j}, defined on $\overline{\Omega_i}$, that is equal to one at the nodal points*

of F_h^j and zero on $\Gamma_{i,h} \setminus F_h^j$, such that

$$\begin{aligned}
&\sum_{F^j \subset \Gamma_i} \theta_{F^j}(\mathbf{x}) = 1, \quad \mathbf{x} \in (\Omega_{i,h} \cup \Gamma_{i,h}) \setminus W_h^i, \\
&0 \le \theta_{F^j} \le 1, \\
&|\nabla \theta_{F^j}| \le C/r, \quad \textit{in } \Omega_i \setminus K_\Omega \\
&|\nabla \theta_{F^j}| \le C/H_i, \quad \textit{in } K_\Omega,
\end{aligned} \tag{26}$$

where $r = r(\mathbf{x})$ is the distance to the closest edge of Ω_i that does not lie on $\partial\Omega$.

Proof. We only need to construct four functions and we will do that by constructing them in the three regions K_{int}, K_{edge}, and K_Ω separately.

We start with the inner region K_{int} and employ a similar construction as in [10, Lem. 3.3.6]:
We further partition Ω_i into eight parallelepipeds by bisecting $\{K_{int}, K^{12}, K^{34}, K_\Omega\}$ with the plane $y = 0$; see Figure 3, left. Let the center C be the common vertex to these parallelepipeds and $\{C^j,\ j = 1, \ldots, 6\}$, be their vertices that belong to the six faces of Ω_i; see Figure 3, right. By connecting the center C with the centers C^j and with the eight vertices of Ω_i, and, for each face, by connecting the point C^j with the four vertices of this face, we can partition Ω_i into twenty-four tetrahedra; see Figure 3, right. By intersecting them with K_{int}, we obtain a partition of K_{int} into eight tetrahedra. We first define a function ϑ_{F^j} associated to the face F^j, defined to be $1/4$ at the center C and $\vartheta_{F^j}(C^l) = \delta_{jl}$ at the centers of the faces. On the segments CC^l, these functions are obtained by linear interpolation of the values at C and C^l; see Figure 3, right. The values inside each subtetrahedron formed by the segment CC^l and one edge of F^l are defined to be constant on the intersection of any plane through that edge, and are given by the value on the segment CC^l. We note that this procedure determines ϑ_{F^j} at all points in Ω_i except on the wirebasket W^i.

We next consider the GLL triangulation $\mathcal{T}_k(\Omega_i)$ and interpolate ϑ_{F^j} at the GLL nodes in $\overline{K}_{int} \setminus W^i$:

$$\theta_{F^j}(\mathbf{x}) = (I^h \vartheta_{F^j})(\mathbf{x}), \qquad \mathbf{x} \in \overline{K}_{int} \setminus W^i.$$

The function θ_{F^j} is set to zero on the nodes in W_h^i. The functions θ_{F^j} are non negative and bounded by one: this proves the second of (26) for points in K_{int}. By construction, also the first of (26) holds for every node in $\overline{K}_{int} \setminus W^i$. The third of (26) can be proven by proceeding in the same way as for [10, Lem. 3.3.6].

We next construct the functions θ_{F^j} in K_{edge}:
We start with K^{12}. We take the values on the common face $\overline{K^{12}} \cap \overline{K}_{int}$ and we extend them as constants into $\overline{K^{12}}$ along the segments parallel to E^1 and E^2; see Figure 3, left. The inequalities in (26) remain valid. We note that the

function obtained is independent of x in K^{12}. A similar construction is carried out in K^{34}.

Finally we construct θ_{F^j} in K_Ω:
We note that K_Ω is divided into two parallelepipeds and that on their internal faces the function θ_{F^j} has already been defined. In addition, θ_{F^j} is bilinear on these faces. It is then enough to assign the value 1/4 at the end points and mid point of the boundary edge and interpolate these values in K_Ω in order to obtain a piecewise trilinear function. The first, second and fourth of (26) follow from standard properties of trilinear functions. □

By examining the proof of the previous lemma, we see that, for an edge E that touches $\partial\Omega$, the value of the functions θ_{F^j} is independent of the coordinate along the direction of E in all the elements of the GLL meshes that touch E_σ; cf. Figure 3, left.

Property 7.2 *Let F be a face of Ω_i and E be an edge, parallel to, say z, that touches $\partial\Omega$. In any element $K_E \in \mathcal{T}_k(\Omega_i)$ that shares an edge with E_σ the function θ_F is independent of z.*

We are now able to bound the face components in the decomposition (20).

Lemma 7.6 *Let θ_{F^j} be the functions in Lemma 7.5, where F^j is a face of the substructure Ω_i. Then, for every $\mathbf{x} \in \Omega_{i,h} \cup \Gamma_{i,h}$ that is not on the wirebasket of Ω_i,*

$$\sum_j I^k(\theta_{F^j} u)(\mathbf{x}) = \sum_j I^h(\theta_{F^j} u)(\mathbf{x}) = u(\mathbf{x}), \quad u \in X_i$$

and

$$|I^k(\theta_{F^j} u)|^2_{1,\Omega_i} \leq C\,(1-\sigma)^{-4} \left(1 + \log\left(\frac{k}{1-\sigma}\right)\right)^2 ||u||^2_{1,\Omega_i}.$$

Proof. We only consider the case of an edge patch Ω_i in full detail; see Figure 3. The proof is similar to that in [40, Lem. 7.8] and [10, Lem. 3.3.7] but particular care is required close to the edges that touch $\partial\Omega$. Indeed, thanks to Lemma 5.1, it is enough to find a bound for the piecewise trilinear function $I^h(\theta_{F^j} u)$.

The first equality follows directly from the first of (26). For the second inequality, we consider an element K, of dimensions h_x, h_y, and h_z, in the GLL mesh $\mathcal{T}_k(\Omega_i)$. We consider three cases (as opposed to [10, Lem. 3.3.7] where only two cases are considered): K may belong to the region K_Ω containing the boundary edge, touch the wirebasket, or may not touch it; see Figure 3.

Case 1. We start with an element that touches an edge E and does not belong to K_Ω. We can proceed as in [10, Lem. 3.3.7] if E does not touch $\partial\Omega$ ($E = E^5$) or, in case it does ($E = E^l$, $l = 1, \ldots, 4$), if K does not touch E_σ. We only consider the case of $E = E^3$ in full detail; cf. Figure 3, left. The nodal values of $I^h(\theta_{F^j} u)$ on K are 0, 0, 0, 0, $u(a)$, $u(b)$, $\theta_{F^j}(c)u(c)$, and $\theta_{F^j}(d)u(d)$,

with a and b vertices on a face and c and d vertices inside Ω_i. It is immediate to see that

$$\begin{aligned} &c(1-\sigma)h_x \leq h_y \leq C(1-\sigma)^{-1}h_x, \\ &h_x \leq C(1-\sigma)^{-1}h_z. \end{aligned} \tag{27}$$

Using Lemma 5.3 and (27), we can easily find

$$\begin{aligned} |I^h(\theta_{F^j}u|^2_{1,K} &\leq C(1-\sigma)^{-2}h_z\left(u(a)^2+u(b)^2+u(c)^2+u(d)^2\right) \\ &\leq C(1-\sigma)^{-2}\left(\int_a^b u^2dz+\int_c^d u^2dz\right), \end{aligned}$$

where we have also used the fact that θ_{F^j} has values between zero and one. Summing over the element K and using in Lemma 7.3 for segments that are parallel to E give

$$\sum_K |I^h(\theta_{F^j}u)|^2_{1,K} \leq C\,(1-\sigma)^{-4}\,(1+\log k)\,\|u\|^2_{1,\Omega_i},$$

where the sum is taken over the elements in $\mathcal{T}_k(\Omega_i)$ that touch an edge E, such that E does not touch $\partial\Omega$ or, if it does, K does not touch E_σ.

We next consider the case where K shares an edge with E_σ. The terms involving the x and y derivatives can be bounded as before: indeed, the first of (27) still holds in this case. However, the second of (27), needed to bound the z derivative, does not hold. Using Lemma 5.3 we find

$$\|\partial_z I^h(\theta_{F^j}u)\|^2_{0,K} \leq C(h_xh_y/h_z)\left((u(a)-u(b))^2+(\theta_{F^j}(c)u(d)-\theta_{F^j}(d)u(d))^2\right).$$

Property 7.1 ensures that $\theta_{F^j}(c)=\theta_{F^j}(d)$ and thus

$$\|\partial_z I^h(\theta_{F^j}u)\|^2_{0,K} \leq C\|\partial_z(\theta_{F^j}u)\|^2_{0,K}.$$

Summing over the elements K that touch E_σ gives

$$\sum_K \|\partial_z(I^h(\theta_{F^j}u)\|^2_{0,K} \leq C\,\|\partial_z(\theta_{F^j}u)\|^2_{0,\Omega_i}$$

and thus

$$\sum_{\overline{K}\cap W^i\neq\emptyset} |I^h(\theta_{F^j}u)|^2_{1,K} \leq C\,(1-\sigma)^{-4}\,(1+\log k)\,\|u\|^2_{1,\Omega_i}. \tag{28}$$

Case 2. We now consider an element $K\in\mathcal{T}_k(\Omega_i)$ that does not touch the wirebasket and does not belong to K_Ω. The proof for this case is similar to that of [10, Lem. 3.3.7]. Using Lemma 5.2 and the second of (26), we have

$$\sum_{\substack{K\subset\Omega_i\setminus K_\Omega \\ \overline{K}\cap W^i=\emptyset}} |I^h(\theta_{F^j}u)|^2_{1,K} \leq C\sum_K(|u|^2_{1,K}+r_K^{-2}\|u\|^2_{0,K}),$$

where r_K is the distance of the baricenter of K from the wirebasket. We have

$$\begin{aligned}\sum_K r_K^{-2}\|u\|_{0,K}^2 &\le C \int\limits_{K_{int}\cup K^{12}\cup K^{34}} r^{-2}u^2 d\mathbf{x} \\ &\le C\int\limits_{K_{int}} r_5^{-2}u^2 d\mathbf{x} + C\sum_{j=1}^{2}\int\limits_{K^{12}\cup K_{int}} r_j^{-2}u^2 d\mathbf{x} + C\sum_{j=3}^{4}\int\limits_{K^{34}\cup K_{int}} r_j^{-2}u^2 d\mathbf{x},\end{aligned}$$

where r_j denotes the distance of a point from the edge E^j and the region consisting of the elements in the GLL mesh $\mathcal{T}_k(\Omega_i)$ that touch the wirebasket is assumed to be excluded from the domains of integration; cf. Figure 3, left. Each of the integrals on the right, associated to an edge $E = E^j$, can be estimated using cylindrical coordinates with the ζ axis coinciding with E^j and the radial direction r_j normal to E^j. We only consider E^5 in detail; cf. Figure 3. The other integrals can be estimated in the same way. If the point V is the intersection between E^5 and the section corresponding to a fixed ζ and K_V is the element of the two-dimensional mesh $\mathcal{T}(\zeta)$ that contains V, we can write

$$\begin{aligned}\int\limits_{K_{int}} r_5^{-2}u^2 d\mathbf{x} &\le C\int\limits_{K_V} r_5^{-2}\,dxdy\int\limits_{-1}^{1} u^2 d\zeta \\ &\le C(1-\sigma)^{-2}(1+\log k)\|u\|_{1,\Omega_i}^2\int\limits_{K_V} r_5^{-2}\,dxdy,\end{aligned}$$

where we have used Lemma 7.3 for the last inequality; cf. Figure 2, right. The last integral can be estimated by

$$\int\limits_{K_V} r_5^{-2}\,dxdy \le C\int_{k^{-2}(1-\sigma)}^{2} r_5^{-1}\,dr_5\int_0^{2\pi} d\phi \le C\left(1+\log\left(\frac{k}{1-\sigma}\right)\right).$$

Considering similar contributions for the other edges, we then find

$$\sum_{\substack{K\subset\Omega_i\setminus K_\Omega\\ \overline{K}\cap W^i=\emptyset}} |I^h(\theta_{F^j}u)|_{1,K}^2 \le C|u|_{1,\Omega_i}^2 + C(1-\sigma)^{-2}\left(1+\log\left(\frac{k}{1-\sigma}\right)\right)^2\|u\|_{1,\Omega_i}^2. \tag{29}$$

Case 3. We are now left with the case $K\subset K_\Omega$. Since, in this case, $|\nabla\theta_{F^j}|$ is bounded by a constant, Lemma 5.2 ensures

$$\sum_{K\subset K_\Omega} |I^h(\theta_{F^j}u)|_{1,K}^2 \le C\,\|u\|_{1,\Omega_i}^2.$$

The proof is concluded by combining this inequality with (28) and (29), and applying Lemma 5.1. □

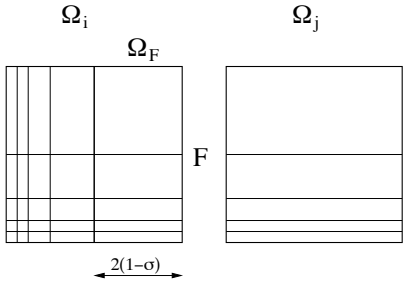

Figure 4: The cross sections of an edge and a face patch, or a corner and an edge patch, with a common face F.

8 Comparison results

In the analysis of many iterative substructuring methods, it is necessary to compare certain norms of discrete harmonic functions on different substructures that have the same trace on a common face, edge, or vertex.

As already pointed out in [40], if the local meshes are shape-regular and quasi-uniform, the comparison for functions on adjacent substructures that have the same value on a common face, can be made using a trace theorem (which is valid for general functions in H^1) and a stable extension. However, the existence of stable extensions for meshes that are not quasi-uniform or shape-regular is far from trivial. For this reason, here we will adopt the same strategy as in [40], since the meshes considered are highly anisotropic but of a particular type.

We note that we only need to consider three cases: that of a face shared by an unrefined and a face patch, by a face and an edge patch, and by an edge and a corner patch. We only consider the last two case in full detail, since the former can be treated in exactly the same way. We consider the two substructures Ω_i and Ω_j in Figure 4, which share the face F. Since we proceed in exactly the same way as in [40, Sect. 7.3], we do not present any proof here. We first consider Ω_i and suppose that it coincides with the reference cube $\hat{Q}$. The face F corresponds to $x = 1$. Let Ω_F be the layer of points in Ω_i within a distance $2(1-\sigma)$ from F.

The following lemma can be proven in the same way as [40, Lem. 7.9].

Lemma 8.1 *Let $u_F \in U_i$ be a face function on Ω_i, i.e, a discrete harmonic function that vanishes on $\partial\Omega_i \setminus F$, and $\tilde{u}_F \in X_i$, such that*

1. *$\tilde{u}_F$ is equal to u_F on F and vanishes on $\partial\Omega_F \setminus F$;*
2. *$\tilde{u}_F$ is discrete harmonic in Ω_F;*
3. *$\tilde{u}_F$ vanishes in $\Omega_i \setminus \Omega_F$.*

Then

$$|u_F|^2_{1,\Omega_i} \leq |\tilde{u}_F|^2_{1,\Omega_i} \leq \|\nabla\theta_{\sigma,F}\|^2_\infty \, |u_F|^2_{1,\Omega_i},$$

where $\theta_{\sigma,F} \in W^{1,\infty}(\Omega_i)$ *is any function that is equal to one on* F*, vanishes in* $\Omega_i \setminus \Omega_F$*, and has values in* $(0,1)$ *in the rest of* Ω_i*. In particular we can find a function such that*

$$\|\nabla\theta_{\sigma,F}\|_\infty \leq C(1-\sigma)^{-1}.$$

The comparison result for face functions can be then found by noting that we can map Ω_j and its mesh into Ω_F and the corresponding local mesh, by a simple dilation in the horizontal direction.

Theorem 8.1 *Let* F *be a face that is common to* Ω_i *and* Ω_j *and* $u_F \in U$ *be a piecewise discrete harmonic function that is identically zero at all nodal points in* $\Gamma_h \setminus F_h$ *. Then,*

$$c\,(1-\sigma)\,|u_F|^2_{1,\Omega_i} \leq |u_F|^2_{1,\Omega_j} \leq C(1-\sigma)^{-1}\,|u_F|^2_{1,\Omega_i}.$$

For vertex and edge functions the following lemma is sufficient for our analysis.

Lemma 8.2 *Let* Ω_i *and* Ω_j *be two substructures and* $u \in X$*. If* $V = V^i = V^j$ *is a common vertex, then the vertex components of* u *satisfy*

$$\|u_{V^j}\|^2_{h,W^j} \leq C(1-\sigma)^{-1}\|u_{V^i}\|^2_{h,W^i}.$$

If $E = E^i = E^j$ *is a common edge, then the edge components of* u *satisfy*

$$\|u_{E^j}\|^2_{h,W^j} \leq C(1-\sigma)^{-2}\|u_{E^i}\|^2_{h,W^i}.$$

Proof. For the first inequality, we note that the modified norms $\|\cdot\|_{h,W^i}$ and $\|\cdot\|_{h,W^j}$ coincide with the L^2 norms, since a vertex function vanishes at all nodal points in Γ_h except at that vertex and we only consider internal vertices. It is enough to compare a contribution from an edge E^j of Ω_j with that of an edge E^i of Ω_i. The worst possible case occurs when E^j does not touch $\partial\Omega$ but E^i does; cf. Figure 4. Let $\phi(\hat{z})$ be the function in $\mathbb{Q}_k(I)$ that vanishes at all the GLL nodes in I, except at -1 where it is equal to $u(V)$. Using the change of variables $z = (1-\sigma)(\hat{z}+1) - 1$ and the fact that u_{V^i} vanishes in E^i_σ, we have

$$\begin{aligned}\int_{E^j} u_{V^j}(\hat{z})^2 d\hat{z} &= \int_{-1}^{1} \phi(\hat{z})^2 d\hat{z} = (1-\sigma)^{-1}\int_{-1}^{-1+2(1-\sigma)} \phi(z)^2 dz \\ &= (1-\sigma)^{-1}\int_{E^i_{1-\sigma}} u_{V^i}(z)^2 dz = (1-\sigma)^{-1}\int_{E^i} u_{V^i}(z)^2 dz.\end{aligned}$$

For the second inequality, it is enough to use the definition of the modified norms $\|\cdot\|_{h,W^i}$ and $\|\cdot\|_{h,W^j}$ and Property 7.1 ∎

9 Proof of Assumption 6.1

We are now ready to give an upper bound for ω in Assumption 6.1. Our proof is similar to that in [31, Lem. 9.1]. We note that if $u_i \in U_i$, its extension $u = R_i^T u_i$ vanishes on Γ_h except at the nodal points in $\Gamma_{i,h}$ and its support is thus contained in the union of Ω_i and its neighboring substructures. In order to estimate ω we thus have to estimate the energy of u in these substructures in terms of the energy of $\mathcal{H}_i(\delta_i u_i)$ in Ω_i alone.

We first note that, by simple calculation, we have

$$\rho_j(\delta_i^\dagger(\mathbf{x}))^2 = \rho_j \delta_i(\mathbf{x})^{-2} \leq \min\{\rho_i, \rho_j\}, \qquad \mathbf{x} \in \Gamma_{i,h}, \quad j \in \mathcal{N}_\mathbf{x}. \tag{30}$$

Let $u_i \in Range(\tilde{P}_i)$. We start with a substructure Ω_j that only has a vertex $V = V^i = V^j$ in common with Ω_i. We note that, according to the decomposition (21), u has only a wirebasket component $u_{V^j} = u$ on Ω_j, which vanishes at all nodes in $\Gamma_{j,h}$ except at V. Using Lemma 7.1, we find

$$a_j(u,u) = \rho_j |u_{V^j}|^2_{1,\Omega_j} \leq C\,\rho_j\,(1-\sigma)^{-2}\,\|u_{V^j}\|^2_{h,W^j} = C\,\rho_j\,\delta_{i,V}^{-2}\,(1-\sigma)^{-2}\,\|\delta_i u_{V^j}\|^2_{h,W^j},$$

where $\delta_{i,V} = \delta_i(V)$. We next note that, thanks to Lemma 8.2, the norm $\|\cdot\|_{h,W^j}$ associated to Ω_j can be bounded by $\|\cdot\|_{h,W^i}$. In addition, we can apply Lemmas 7.4 and 7.2 and find

$$\begin{aligned}
\rho_i\|\delta_i u_{V^j}\|^2_{h,W^j} &\leq C(1-\sigma)^{-1}\rho_i\|(\delta_i u_i)_{V^i}\|^2_{h,W^i} \leq C(1-\sigma)^{-1}\rho_i\|\mathcal{H}_i(\delta_i u_i)\|^2_{h,W^i} \\
&\leq C(1-\sigma)^{-3}(1+\log k)\;\rho_i\|\mathcal{H}_i(\delta_i u_i)\|^2_{1,\Omega_i} \\
&= C(1-\sigma)^{-3}(1+\log k)\;(a_i(\mathcal{H}_i(\delta_i u_i),\mathcal{H}_i(\delta_i u_i)) + \rho_i H_i^{-2}\|\mathcal{H}_i(\delta_i u_i)\|^2_{0,\Omega_i}).
\end{aligned}$$

The L^2 component in the last term can be bounded by the local bilinear form $a_i(\cdot,\cdot)$, thanks to a Poincaré inequality for floating subdomains (cf. (19)), or thanks to a Friedrichs inequality for substructures that touch $\partial\Omega$. Combining these two estimates and using (30), we find

$$a_j(u,u) = a_j(u_{V^j}, u_{V^j}) \leq C(1-\sigma)^{-5}(1+\log k)\;a_i(\mathcal{H}_i(\delta_i u_i),\mathcal{H}_i(\delta_i u_i)). \tag{31}$$

We next consider a substructure Ω_j that only has an edge $E = E^i = E^j$ in common with Ω_i, with vertices $V^{j1} = V^{i1}$ and $V^{j2} = V^{i2}$. We note that, according to the decompositions (20) and (21), u has only a wirebasket component on Ω_j,

$$u = u_{W^j} = u_{V^{j1}} + u_{V^{j2}} + u_{E^j},$$

which vanishes at all nodes in $\Gamma_{j,h}$ except at those on the closure $\overline{E^j}$. We then have

$$a_j(u,u) \leq 3a_j(u_{V^{j1}}, u_{V^{j1}}) + 3a_j(u_{V^{j2}}, u_{V^{j2}}) + 3a_j(u_{E^j}, u_{E^j}).$$

For the two vertex components, we can proceed as before and find similar bounds to (31). For the edge component, we use Lemma 7.1, the definition of $\|\cdot\|_{h,E^j}$,

and the fact that δ_i is constant at all the nodal points in E_h. We find

$$a_j(u_{E^j}, u_{E^j}) = \rho_j |u_{E^j}|^2_{1,\Omega_j} \leq C \, \frac{\rho_j}{(1-\sigma)^2} \, \|u_{E^j}\|^2_{h,E^j} \leq C \, \frac{\rho_j \, \delta^{-2}_{i,E}}{(1-\sigma)^2} \, \|\delta_i u_{E^j}\|^2_{h,E^j},$$

where $\delta_{i,E}$ is the constant value of δ_i on E. Thanks to Lemma 8.2, the norm $\|\cdot\|_{h,E^j}$ associated to Ω_j can be bounded by $\|\cdot\|_{h,E^i}$. In addition, we can apply Lemmas 7.4 and 7.2 and find

$$\begin{aligned}
\rho_i \|\delta_i u_{E^j}\|^2_{h,E^j} &\leq C(1-\sigma)^{-2} \rho_i \|(\delta_i u_i)_{E^i}\|^2_{h,E^i} \leq C(1-\sigma)^{-2} \rho_i \|\mathcal{H}_i(\delta_i u_i)\|^2_{h,E^i} \\
&\leq C(1-\sigma)^{-4}(1+\log k)\, \rho_i \|\mathcal{H}_i(\delta_i u_i)\|^2_{1,\Omega_i} \\
&= C(1-\sigma)^{-4}(1+\log k)\, (a_i(\mathcal{H}_i(\delta_i u_i), \mathcal{H}_i(\delta_i u_i)) + \rho_i H_i^{-2} \|\mathcal{H}_i(\delta_i u_i)\|^2_{0,\Omega_i}).
\end{aligned}$$

As before, the L^2 component in the last term can be bounded by the local bilinear form $a_i(\cdot,\cdot)$, thanks to a Poincaré or a Friedrichs inequality. Combining these two estimates and using (30), we find

$$a_j(u_{E^j}, u_{E^j}) \leq C(1-\sigma)^{-6}(1+\log k)\, a_i(\mathcal{H}_i(\delta_i u_i), \mathcal{H}_i(\delta_i u_i)). \tag{32}$$

We next consider a substructure Ω_j that shares a face F and thus also the edges and vertices that lie on ∂F. We note that on Ω_j, u can be decomposed as

$$u = u_{W^j} + u_F.$$

We have

$$a_j(u,u) = \rho_j |u|^2_{1,\Omega_j} \leq 2\rho_j (|u_{W^j}|^2_{1,\Omega_j} + |u_F|^2_{1,\Omega_j}).$$

The wirebasket component can be bounded as before; cf. (31) and (32). For the face component we first note that the function δ_i is equal to a constant value $\delta_{i,F}$ at all nodal points inside F. Using (30), we can then write

$$\rho_j |u_F|^2_{1,\Omega_j} = \rho_j \delta^{-2}_{i,F} \, |\mathcal{H}_j(\delta_i u_F)|^2_{1,\Omega_j} \leq \rho_i |\mathcal{H}_j(\delta_i u_F)|^2_{1,\Omega_j}.$$

Using Corollary 8.1 and Lemma 7.6 yields

$$|\mathcal{H}_j(\delta_i u_F)|^2_{1,\Omega_j} \leq C(1-\sigma)^{-1} |\mathcal{H}_i(\delta_i u_F)|^2_{1,\Omega_i} \leq C(1-\sigma)^{-5} \left(1 + \log\left(\frac{k}{1-\sigma}\right)\right)^2 ||u||^2_{1,\Omega_i}.$$

Combining the last two estimates and using a Poincaré or a Friedrichs inequality, we find

$$a_j(u_F, u_F) \leq C\,(1-\sigma)^{-5} \, \left(1 + \log\left(\frac{k}{1-\sigma}\right)\right)^2 \, a_i(\mathcal{H}_i(\delta_i u), \mathcal{H}_i(\delta_i u)). \tag{33}$$

We finally need to consider the energy of u in Ω_i, $a_i(u,u)$. We note that we can decompose u on Ω_i according to (20). The wirebasket and the face components

can be bounded as before. Summing over i and the neighboring subdomains, we then find

$$a(u,u) \leq \frac{C}{(1-\sigma)^6}\left(1+\log\left(\frac{k}{1-\sigma}\right)\right)^2\left(\sum_{V^{ij}}1+\sum_{E^{ij}}1+\sum_{F^{ij}}1\right)a_i(\mathcal{H}_i(\delta_i u),\mathcal{H}_i(\delta_i u)).$$

Since the partition $\mathcal{T}_m$ is shape-regular, the number of subdomains to which an edge or a vertex may belong is bounded. We finally obtain

$$\omega \leq C\,(1-\sigma)^{-6}\,\left(1+\log\left(\frac{k}{1-\sigma}\right)\right)^2.$$

Since in practice σ is bounded away from one, we obtain the same bound as for Neumann-Neumann methods for p finite element approximations on shape-regular meshes

$$\kappa(P_{NN}) \leq C\,(1+\log k)^2;$$

see, e.g., [30]. We stress the fact that the constants in the last two estimates are independent of the coefficients ρ_i and the refinement level n (and thus of the aspect ratio of the mesh $\mathcal{T}_{bl}^{n,\sigma}$).

10 Numerical results

The purpose of this section is to present some numerical experiments in order to validate our analysis on some medium-size problems. An extensive numerical study is presented elsewhere; see [41].

We consider approximations on the unit cube $\Omega = (0,1)^3$. We choose $\rho \equiv 1$ and the right-hand side $f \equiv 1$. The macromesh $\mathcal{T}_m$ consists of $N \times N \times N$ cubic substructures. Geometric refinement is performed towards the three edges $x = 0$, $y = 0$, and $z = 0$, with $\sigma = 0.5$; see Figure 5, left. Given a polynomial degree k, we choose $n = k$ as is required for robust exponential convergence; see, e.g., [4, 5]. The conjugate gradient iteration is stopped after a reduction of the Euclidean norm of the initial residual of 10^{-14}.

We note that even for moderate values of k and N, extremely large linear systems are obtained; cf. Tables 1 and 2. Huge local blocks need to be inverted, both for the application of S (solution of local Dirichlet problems) and the preconditioner (solution of local Neumann problems). Due to memory limitations in our Matlab implementation, we have employed approximate solvers for local Dirichlet and Neumann problems. We refer to [39, Sect. 4.4] for details on the implementation. In particular, we have used a conjugate gradient iteration with an incomplete Cholesky factorization with drop tolerance 10^{-3} for all local problems. The iteration is stopped after a reduction of the initial residual of a factor 10^{-3} or after 20 iteration steps. Our numerical results show that the theoretical bounds for the case of exact solvers in Lemma 6.2 remain valid in this case; cf. Tables 1 and 2.

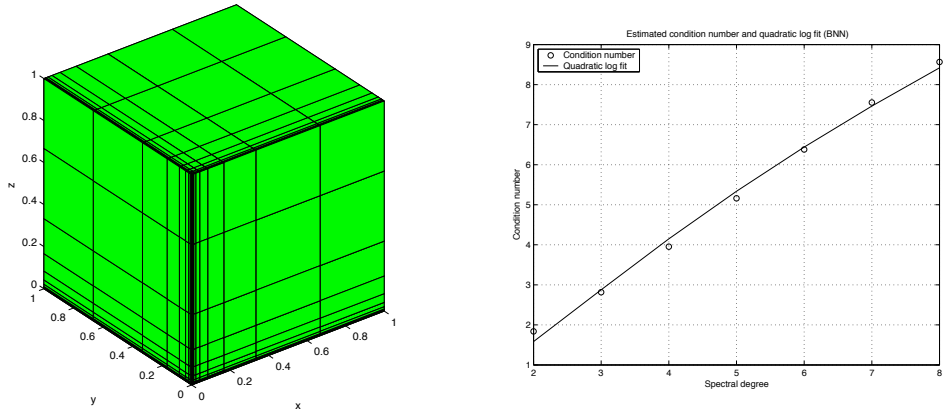

Figure 5: Geometric refinement towards one corner ($N = 3$, $\sigma = 0.5$, and $n = 6$), left, and estimated condition numbers (circles) from Table 1 and least-square second order logarithmic polynomial fit (solid line) versus k, right.

For a fixed partition into substructures with $N = 3$, Table 1 shows the size of the original problem, the iteration count, the estimated maximum and minimum eigenvalues, and the condition number for different values of k. We note that the minimum eigenvalue is close to one; see Lemma 6.2. In addition a moderate growth of the maximum eigenvalue is observed with k; such growth is consistent with the quadratic bound in Lemma 6.3; see Figure 5, right.

We next consider the same problem, and fix the polynomial degree $k = 4$. Table 2 shows the results for different values of N. The iteration counts, and the smallest and largest eigenvalues appear to be bounded independently of the number of subdomains.

11 Concluding remarks

As for the analysis in [40], some important issues still need to be addressed. We refer to our previous work for a full discussion of these issues.

Our analysis is restricted to approximations that employ nodal basis functions on the Gauss-Lobatto nodes. Indeed, for three-dimensional shape-regular meshes good performance of iterative substructuring methods is in general ensured only if these basis functions are employed and for more general p or hp version finite element approximations many important issues remain to be solved even for shape-regular meshes; see, e.g., [38] and the references therein.

The Dirichlet and Neumann problems that we need to solve (cf. S_i and $S_i^\dagger$) can be potentially very large. Approximate local solvers can be employed

Fixed number of subdomains ($N = 3$)					
NN (inexact)					
k	$size$	It	λ_{max}	λ_{min}	κ
2	1331	15	1.8379	1	1.8379
3	6859	20	2.8165	0.99997	2.8166
4	24389	25	3.9507	0.99947	3.9528
5	68921	29	5.1507	0.99799	5.1611
6	166375	34	6.3675	0.99801	6.3803
7	357911	38	7.5082	0.99395	7.554
8	704969	40	8.5298	0.99574	8.5663

Table 1: Conjugate Gradient method for the Schur complement system with Neumann-Neumann preconditioner with inexact solvers: iteration counts, maximum and minimum eigenvalues, and condition numbers, versus the polynomial degree, for the case of a fixed partition. The size of the original problem is also reported.

for iterative substructuring methods (see, e.g., [39, 16]) and some have been proposed in [18] for *hp* approximations. In our numerical experiments, we have employed a conjugate gradient iteration with an incomplete Choleski preconditioner, however, we believe that the tensor product structure of corner, edge, and face patches can be exploited. This is left to a future work.

We believe that the analysis and/or the development of iterative substructuring methods for general meshes with hanging nodes still need to be fully addressed. These meshes are widely used in practice. There is no straightforward way of defining Neumann-Neumann or FETI algorithms when hanging nodes lie on the interface Γ; see [40, Rem. 6.1] for more details.

Finally, our analysis has been carried out for the model problem (1), which indeed does not exhibit boundary layers. As for two-dimensional problems in [40, 42], numerical results show that our algorithms are robust when applied to certain singularly perturbed problems. Extensive numerical results will be presented in [41].

Acknowledgments

The authors are grateful to Christoph Schwab and Olof Widlund for enlightening discussions of their work.

Fixed spectral degree $k = 4$					
NN (inexact)					
N	$size$	It	λ_{max}	λ_{min}	κ
2	15625	18	2.6417	0.99929	2.6436
3	24389	25	3.9507	0.99947	3.9528
4	35937	28	4.1084	0.99934	4.1111
5	50653	29	4.1378	0.9994	4.1402
6	68921	30	4.1492	0.99945	4.1515
7	91125	30	4.1555	0.99952	4.1575
8	117649	30	4.1593	0.99955	4.1612
9	148877	30	4.1618	0.99962	4.1634
10	185193	30	4.1636	0.9997	4.1648

Table 2: Conjugate Gradient method for the Schur complement system with Neumann-Neumann preconditioner with inexact solvers: iteration counts, maximum and minimum eigenvalues, and condition numbers, versus the number of substructures, for the case of a fixed polynomial degree and partitions into $N \times N \times N$ substructures. The size of the original problem is also reported.

References

[1] Mark Ainsworth. A hierarchical domain decomposition preconditioner for *h-p* finite element approximation on locally refined meshes. *SIAM J. Sci. Comput.*, 17(6):1395–1413, 1996.

[2] Mark Ainsworth. A preconditioner based on domain decomposition for *hp*–FE approximation on quasi–uniform meshes. *SIAM J. Numer. Anal.*, 33:1358–1376, 1996.

[3] Mark Ainsworth and Spencer Sherwin. Domain decomposition preconditioners for *p* and *hp* finite element approximation of Stokes equations. *Comp. Methods Appl. Mech. Eng.*, 175:243–266, 1999.

[4] B. Andersson, U. Falk, I. Babuška, and T. von Petersdorff. Reliable stress and fracture mechanics analysis of complex aircraft components using a *hp*–version FEM. *Int. J. Numer. Meth. Eng.*, 38(13):2135–2163, 1995.

[5] Ivo Babuška and Benqi Guo. Approximation properties of the *hp*–version of the finite element method. *Comp. Methods Appl. Mech. Eng.*, 133:319–346, 1996.

[6] Christine Bernardi and Yvon Maday. Spectral methods. In *Handbook of Numerical Analysis, Vol. V, Part 2*, pages 209–485. North-Holland, Amsterdam, 1997.

[7] Manoj Bhardwaj, David Day, Charbel Farhat, Michel Lesoinne, Kendall Pierson, and Daniel Rixen. Application of the FETI method to ASCI problems: Scalability results on one thousand processors and discussion of highly heterogeneous problems. *Int. J. Numer. Meth. Engng.*, 47:513–535, 2000.

[8] Ion Bica. *Iterative substructuring algorithms for the p–version finite element method for elliptic problems*. PhD thesis, Courant Institute, New York University, 1997.

[9] Claudio Canuto. Stablization of spectral methods by finite element bubble functions. *Comput. Methods Appl. Mech. Engrg*, 116:13–26, 1994. Proceedings of ICOSAHOM 92, a conference held in Montpellier, France, June 1992.

[10] Mario A. Casarin. *Schwarz Preconditioners for Spectral and Mortar Finite Element Methods with Applications to Incompressible Fluids*. PhD thesis, Courant Institute of Mathematical Sciences, March 1996. Tech. Rep. 671, Department of Computer Science, New York University, `URL: file://cs.nyu.edu/pub/tech-reports/tr717.ps.gz`.

[11] Maksymilian Dryja, Marcus V. Sarkis, and Olof B. Widlund. Multilevel Schwarz methods for elliptic problems with discontinuous coefficients in three dimensions. *Numer. Math.*, 72(3):313–348, 1996.

[12] Maksymilian Dryja and Olof B. Widlund. Schwarz methods of Neumann-Neumann type for three-dimensional elliptic finite element problems. *Comm. Pure Appl. Math.*, 48(2):121–155, February 1995.

[13] Charbel Farhat and François-Xavier Roux. Implicit parallel processing in structural mechanics. In J. Tinsley Oden, editor, *Computational Mechanics Advances*, volume 2 (1), pages 1–124. North-Holland, 1994.

[14] Benqi Guo and Weiming Cao. Additive Schwarz methods for the *hp* version of the finite element method in two dimensions. *SIAM Journal on Scientific Computing*, 18(5):1267–1288, 1997.

[15] Benqi Guo and Weiming Cao. An additive Schwarz method for the *hp*–version of the finite element method in three dimensions. *SIAM J. Numer. Anal.*, 35:632–654, 1998.

[16] Axel Klawonn and Olof B. Widlund. A domain decomposition method with Lagrange multipliers and inexact solvers for linear elasticity. *SIAM J. Sci. Comput.*, 22(4):1199–1219, October 2000.

[17] Axel Klawonn and Olof B. Widlund. FETI and Neumann-Neumann iterative substructuring methods: connections and new results. *Comm. Pure Appl. Math.*, 54(1):57–90, 2001.

[18] V. Korneev, J.E. Flaherty, J.T. Oden, and J. Fish. Additive Schwarz algorithms for solving hp-version finite element systems on triangular meshes. *SIAM J. Numer. Anal.*, 1998. submitted.

[19] Patrick Le Tallec. Domain decomposition methods in computational mechanics. In J. Tinsley Oden, editor, *Computational Mechanics Advances*, volume 1 (2), pages 121–220. North-Holland, 1994.

[20] Patrick Le Tallec and Abani Patra. Non–overlapping domain decomposition methods for adaptive *hp* approximations of the Stokes problem with discontinuous pressure fields. *Comp. Methods Appl. Mech. Eng.*, 145:361–379, 1997.

[21] Jan Mandel. Efficient domain decomposition preconditioning for the p-version finite element method in three dimensions. Technical report, Computational Mathematics Group, University of Colorado at Denver, 1989.

[22] Jan Mandel. Hierarchical preconditioning and partial orthogonalization for the p-version finite element method. In Tony F. Chan, Roland Glowinski, Jacques Périaux, and Olof Widlund, editors, *Third International Symposium on Domain Decomposition Methods for Partial Differential Equations*, Philadelphia, PA, 1990. SIAM. Held in Houston, Texas, March 20-22, 1989.

[23] Jan Mandel. Two-level domain decomposition preconditioning for the p-version finite element version in three dimensions. *Int. J. Numer. Meth. Eng.*, 29:1095–1108, 1990.

[24] Jan Mandel and Marian Brezina. Balancing domain decomposition for problems with large jumps in coefficients. *Math. Comp.*, 65:1387–1401, 1996.

[25] Jens Markus Melenk. On condition numbers in *hp*-FEM with Gauss-Lobatto-based shape functions. *J. Comput. Appl. Math.*, 139(1):21–48, 2002.

[26] Jens Markus Melenk and Christoph Schwab. *hp*–FEM for reaction–diffusion equations. I: Robust exponential convergence. *SIAM J. Numer. Anal.*, 35:1520–1557, 1998.

[27] Jindřich Nečas. *Les méthodes directes en théorie des équations elliptiques*. Academia, Prague, 1967.

[28] J. T. Oden, Abani Patra, and Yusheng Feng. Parallel domain decomposition solver for adaptive *hp* finite element methods. *SIAM J. Numer. Anal.*, 34:2090–2118, 1997.

[29] Luca F. Pavarino. Additive Schwarz methods for the p-version finite element method. *Numer. Math.*, 66(4):493–515, 1994.

[30] Luca F. Pavarino. Neumann-Neumann algorithms for spectral elements in three dimensions. *RAIRO Mathematical Modelling and Numerical Analysis*, 31:471–493, 1997.

[31] Luca F. Pavarino. Preconditioned mixed spectral element methods for elasticity and Stokes problems. *SIAM Journal on Scientific Computing*, 19(6):1941–1957, 1998.

[32] Luca F. Pavarino and Tim Warburton. Overlapping Schwarz methods for unstructured spectral elements. *J. Comput. Phys.*, 160 (1):298–317, 2000.

[33] Luca F. Pavarino and Olof B. Widlund. A polylogarithmic bound for an iterative substructuring method for spectral elements in three dimensions. *SIAM J. Numer. Anal.*, 33(4):1303–1335, August 1996.

[34] Luca F. Pavarino and Olof B. Widlund. Iterative substructuring methods for spectral elements: Problems in three dimensions based on numerical quadrature. *Computers Math. Applic.*, 33(1/2):193–209, January 1997.

[35] Marcus V. Sarkis. *Schwarz Preconditioners for Elliptic Problems with Discontinuous Coefficients Using Conforming and Non-Conforming Elements*. PhD thesis, Courant Institute, New York University, September 1994. TR671, Department of Computer Science, New York University, `URL: file://cs.nyu.edu/pub/tech-reports/tr671.ps.Z`.

[36] Christoph Schwab and Manil Suri. The p and hp version of the finite element method for problems with boundary layers. *Math. Comp.*, 65:1403–1429, 1996.

[37] Christoph Schwab, Manil Suri, and Christos A. Xenophontos. The hp–FEM for problems in mechanics with boundary layers. *Comp. Methods Appl. Mech. Eng.*, 157:311–333, 1998.

[38] Spencer J. Sherwin and Mario A. Casarin. Low energy bases preconditioning for elliptic substructured solvers based on spectral/hp element discretizations. *J. Comput. Phys.*, 171:1–24, 2001.

[39] Barry F. Smith, Petter E. Bjørstad, and William D. Gropp. *Domain Decomposition: Parallel Multilevel Methods for Elliptic Partial Differential Equations*. Cambridge University Press, 1996.

[40] Andrea Toselli and Xavier Vasseur. Neumann-Neumann and FETI preconditioners for *hp*-approximations on geometrically refined boundary layer meshes in two dimensions. Technical Report 02–15, Seminar für Angewandte Mathematik, ETH, Zürich, 2002. Submitted to Numerische Mathematik.

[41] Andrea Toselli and Xavier Vasseur. A numerical study on Neumann-Neumann and FETI methods for hp-approximations on geometrically refined boundary layer meshes II: Three-dimesnional problems. In preparation, 2002.

[42] Andrea Toselli and Xavier Vasseur. A numerical study on Neumann-Neumann and FETI methods for hp-approximations on geometrically refined boundary layer meshes in two dimensions. Technical Report 02–20, Seminar für Angewandte Mathematik, ETH, Zürich, 2002. Submitted to Comput. Meth. Appl. Mech. and Eng.

Research Reports

No.	Authors	Title
03-01	A. Toselli, X. Vasseur	Domain decomposition preconditioners of Neumann-Neumann type for *hp*-approximations on boundary layer meshes in three dimensions
02-26	M. Savelieva	Theoretical study of axisummetrical triple flame
02-25	D. Schötzau, C. Schwab, A. Toselli	Mixed *hp*-DGFEM for incompressible flows III: Pressure stabilization
02-24	F.M. Buchmann, W.P. Petersen	A stochastically generated preconditioner for stable matrices
02-23	A.W. Rüegg, A. Schneebeli, R. Lauper	Generalized *hp*-FEM for Lattice Structures
02-22	L. Filippini, A. Toselli	*hp* Finite Element Approximations on Non-Matching Grids for the Stokes Problem
02-21	D. Schötzau, C. Schwab, A. Toselli	Mixed *hp*-DGFEM for incompressible flows II: Geometric edge meshes
02-20	A. Toselli, X. Vasseur	A numerical study on Neumann-Neumann and FETI methods for *hp*-approximations on geometrically refined boundary layer meshes in two dimensions
02-19	D. Schötzau, Th.P. Wihler	Exponential convergence of mixed *hp*-DGFEM for Stokes flow in polygons
02-18	P.-A. Nitsche	Sparse approximation of singularity functions
02-17	S.H. Christiansen	Uniformly stable preconditioned mixed boundary element method for low-frequency electromagnetic scattering
02-16	S.H. Christiansen	Mixed boundary element method for eddy current problems
02-15	A. Toselli, X. Vasseur	Neumann-Neumann and FETI preconditioners for *hp*-approximations on geometrically refined boundary layer meshes in two dimensions
02-14	Th.P. Wihler	Locking-Free DGFEM for Elasticity Problems in Polygons
02-13	S. Beuchler, R. Schneider, C. Schwab	Multiresolution weighted norm equivalences and applications
02-12	M. Kruzik, A. Prohl	Macroscopic modeling of magnetic hysteresis
02-11	A.-M. Matache, C. Schwab, T. von Petersdorff	Fast deterministic pricing of options on Lévy driven assets